

# Coexistence of Two Bifurcation Regimes in a Closed Ferriin-Catalyzed Belousov–Zhabotinsky Reaction

Jichang Wang,<sup>\*,†</sup> Jinpei Zhao,<sup>†</sup> Yu Chen,<sup>†</sup> Qingyu Gao,<sup>\*,‡</sup> and Yumei Wang<sup>‡</sup>

Department of Chemistry and Biochemistry, The University of Windsor, Windsor, ON N9B 3P4, Canada, and College of Chemical Engineering, China University of Mining and Technology, Xuzhou, Jiangsu Province, 221008, People's Republic of China

Received: September 26, 2004; In Final Form: November 27, 2004

The ferriin-catalyzed Belousov–Zhabotinsky (BZ) reaction was studied in a batch reactor under anaerobic conditions and was found to evolve through two separated regimes of complex oscillations. Significantly, the two bifurcation regimes exhibited qualitatively different dependence on compositions of the reaction mixture, i.e., initial concentrations of bromate, sulfuric acid, malonic acid, and ferriin. The reaction temperature also showed opposite effects on the two bifurcation regimes, in which complexities of the first bifurcation regime were enhanced while oscillations in the second bifurcation regime became simpler as a result of decreasing temperature. Numerical simulations with a 12-variable model developed specifically for the ferriin-BZ system were able to reproduce transient complex oscillations observed in experiments. These calculations further illustrated that reactions such as ferriin and HOBr, ferriin and HBrO<sub>2</sub>, and ferriin and Br<sup>-</sup> were not essential in describing complex dynamics of the ferriin-BZ reaction.

## 1. Introduction

The study of nonlinear chemical dynamics has flourished in the past four decades,<sup>1–6</sup> which led to the observation of a variety of nonlinear spatial and temporal behaviors in various chemical and biochemical reactions.<sup>7–16</sup> The striking color changes between oxidized and reduced states in the Belousov–Zhabotinsky (BZ) reaction (due to the presence of metal catalysts such as Ru(bpy)<sub>3</sub><sup>3+</sup>/Ru(bpy)<sub>3</sub><sup>2+</sup> and Fe(phen)<sub>3</sub><sup>3+</sup>/Fe(phen)<sub>3</sub><sup>2+</sup>) provided a convenient way to investigate pattern formation in a spatially extended medium.<sup>17–28</sup> As a result, despite the discovery of numerous new chemical oscillators in the past two decades, the BZ reaction remains a prototype model in studies of nonlinear dynamics.<sup>17–42</sup>

Mechanisms of the BZ reaction have been understood largely based on the Field–Körös–Noyes (FKN) theory, which was developed to account for the behavior observed primarily in the cerium-catalyzed BZ reaction.<sup>34</sup> In recent studies, however, Gaspar and co-workers showed that, when ferriin was used as the metal catalyst, the behavior of the BZ reaction could not be accounted by simply modifying rate constants of a few elementary steps of the FKN theory.<sup>35</sup> They suggested that possible reactions between ferriin and bromide and between ferriin and bromine, HOBr, etc. should also be considered in the model developed specifically for the ferriin-catalyzed BZ system.<sup>35,36</sup>

To shed light on the understanding of the ferriin-catalyzed BZ reaction mechanism, in this study we systematically characterized the dynamic behavior of the ferriin-BZ reaction in a batch reactor under anaerobic conditions. Our attention was particularly focused on searching for new transient complex oscillations in the above system, because complex oscillations

are extremely susceptible to variations of reaction parameters and thus have particular advantages in characterizing the underlying reaction mechanism. Transient complex oscillations including consecutive period-doubling bifurcations, torus oscillations, and transient chaos have been reported earlier in the cerium-catalyzed BZ reaction.<sup>37–39</sup> In the closed ferriin-catalyzed BZ reaction, only mixed-mode oscillations were reported by Strizhak and co-workers.<sup>40</sup> As shown in the following, this study revealed that the ferriin-catalyzed BZ system was capable of exhibiting two isolated bifurcation regimes even under closed reaction conditions, which resembled the two bifurcation regions observed, respectively, at high and low flow rates in a continuous flow stirred tank reactor (CSTR).<sup>29,30</sup> The mixed-mode oscillations reported earlier by Strizhak and co-workers appeared to correspond to the complex behavior that occurred within the first bifurcation regime in this study. Notably, period-doubled oscillations in the second bifurcation regime lasted for as long as 5 h and thus could be conveniently employed to investigate pattern formation under period-doubled oscillation dynamics.<sup>43,44</sup>

## 2. Experimental Procedures

All reactions were carried out in a thermostated glass vessel, where the temperature was controlled at 20.0 ± 0.1 °C by a circulating water bath (NatLab, RTE 10). Reactions were followed by a platinum electrode coupled with a Hg|Hg<sub>2</sub>SO<sub>4</sub>|K<sub>2</sub>SO<sub>4</sub> reference electrode. The potential was recorded with a personal computer connected through an electrochemistry station, VoltaLab 10 (Radiometer). A bromide ion selective electrode (Orion, 9435BN) coupled with the calomel reference electrode was also employed to follow the evolution of the reaction, and qualitatively the same behavior was observed. Stock solutions of 1.0 M NaBrO<sub>3</sub> (Aldrich, 99%), 0.8 M malonic acid (Aldrich, 98%), and 3 M sulfuric acid (Aldrich, 98%) were dissolved in double distilled water. Ferriin, 0.025 M, was prepared with FeSO<sub>4</sub>·7H<sub>2</sub>O (Aldrich) and 1,10-phenanthroline

\* Corresponding authors. Fax, (519) 973-7098; e-mail, jwang@uwindsor.ca (J.W.). Fax, 86-516-3995758; e-mail, gaoqy@cumt.edu.cn (Q.G.).

<sup>†</sup> The University of Windsor.

<sup>‡</sup> China University of Mining and Technology.

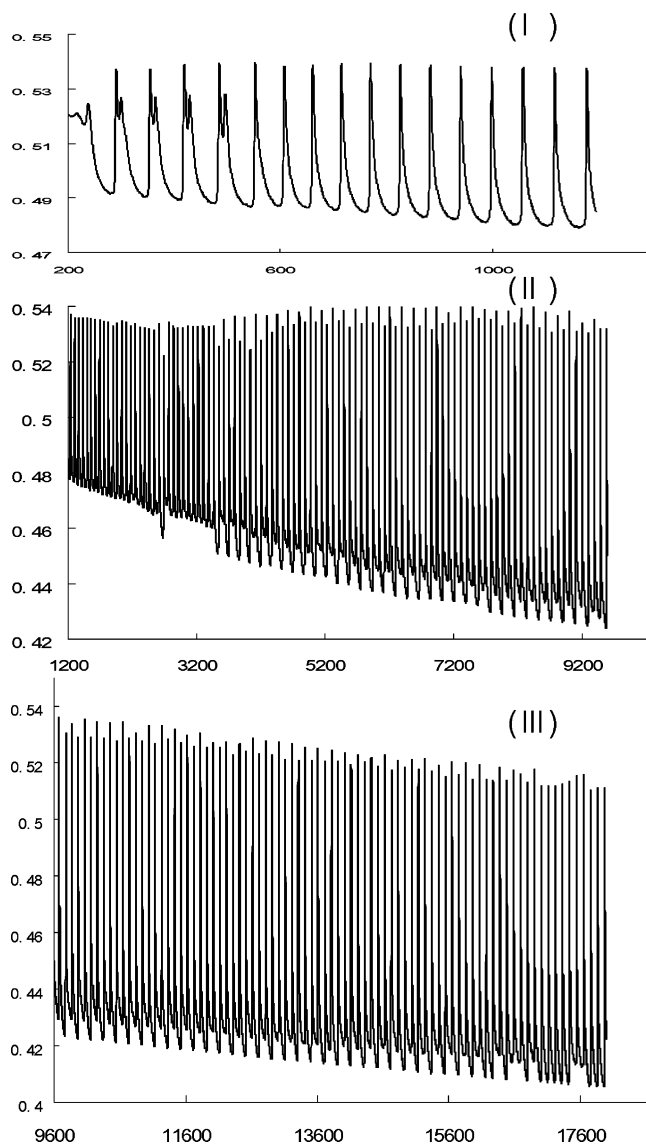


**Figure 1.** Time series showing evolution of ferrioin-catalyzed Belousov–Zhabotinsky reaction in a closed system. Initial compositions of the reaction mixture are  $[\text{H}_2\text{SO}_4] = 0.38 \text{ M}$ ,  $[\text{MA}] = 0.30 \text{ M}$ ,  $[\text{ferrioin}] = 5.0 \times 10^{-4} \text{ M}$ , and  $[\text{BrO}_3^-] = 0.10 \text{ M}$ .

(Aldrich) according to a 1:3 stoichiometric relationship. All chemicals were used in their commercial grade without further purification.

The volume of the reaction mixture was kept constant at 30.0 mL throughout this study. There was about 1 cm gap between the solution and the bottom of the lid. To avoid the influence of oxygen, nitrogen gas was continuously flowed into the gap at a speed of about 0.05 L/min. To examine any kinetic influence imposed by the flow of nitrogen gas, argon was occasionally used at a much lower flow rate ( $<0.01 \text{ L/min}$ ). No difference in the reaction behavior was recorded there. To reduce the amount of oxygen presented initially in these stock solutions, sodium bromate, malonic acid, and sulfuric acid were mixed first in the reactor and the mixture was stirred for 15 min under nitrogen environment.

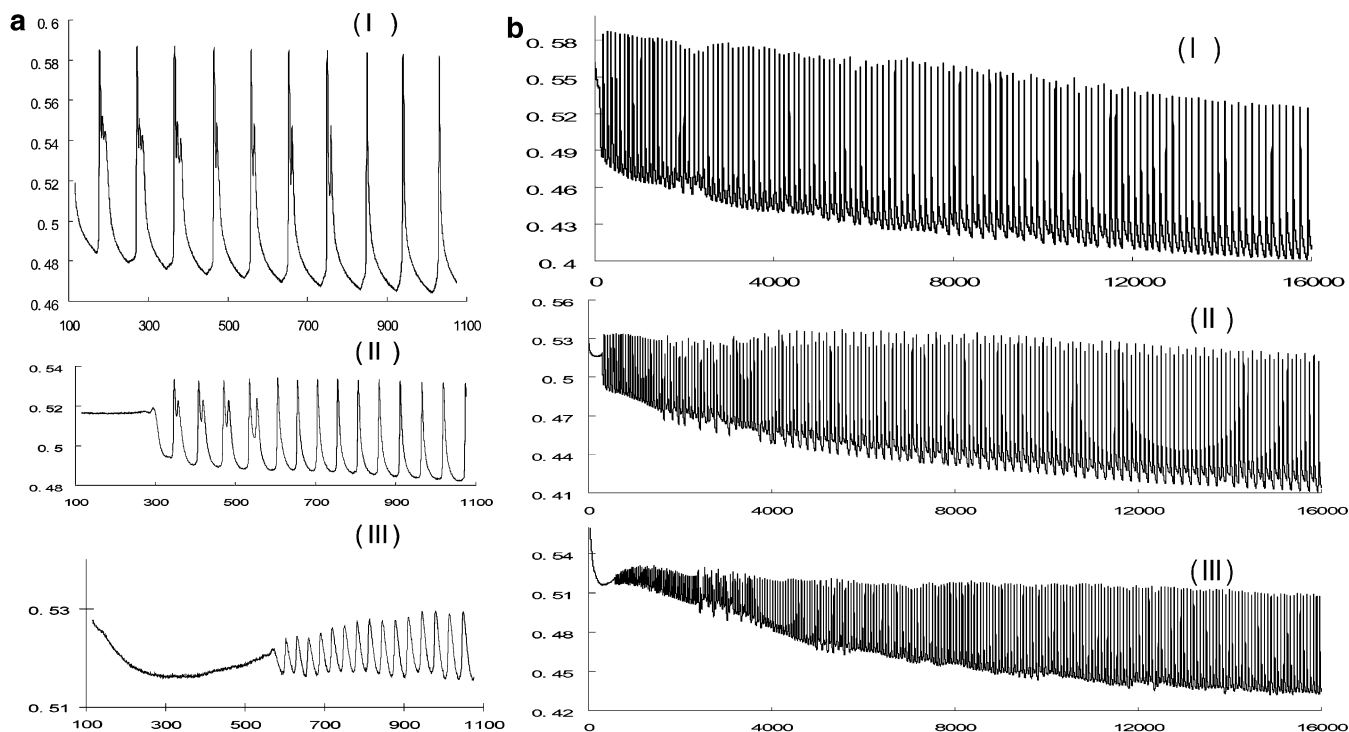
### 3. Experimental Results

Figure 1 presents a time series obtained under the following initial compositions:  $[\text{H}_2\text{SO}_4] = 0.38 \text{ M}$ ,  $[\text{MA}] = 0.30 \text{ M}$ ,  $[\text{ferrioin}] = 5.0 \times 10^{-4} \text{ M}$ , and  $[\text{BrO}_3^-] = 0.10 \text{ M}$ . As reported in earlier investigations,<sup>1</sup> there was a short induction period

before spontaneous oscillations emerged. Interestingly, within the first 500 s every large peak was followed by a small peak, resembling the mode of mixed mode oscillations. As the amplitude of these small peaks increased in time, the BZ reaction smoothly evolved into simple period-1 oscillations. Similar phenomena have been reported earlier by Strizhak and co-workers under quite different reaction conditions, where concentrations of malonic acid and bromate were almost twice as high as those used in this study.<sup>40</sup> Significantly, period-doubled oscillations appeared again at about  $t = 3200 \text{ s}$ , followed by other modes of complex oscillations. In contrast to the short lifetime of the first group of period-doubled oscillations, the second bifurcation sequence lasted for more than 4 h. Between the two regimes of complex oscillations, there was a period of simple period-1 oscillations (ca. 30 min). Note that, unlike in a CSTR, where a bifurcation parameter such as flow rate can be well-defined, in a batch reactor everything is transient except the final thermodynamic equilibrium state. Nevertheless, concentrations of initial reactants in a batch reaction could be viewed as a bifurcation control parameter, which decreases continuously in time. If the decrease in the concentration of reactants is slow enough, which corresponds to slowly varying the bifurcation parameter such as flow rate in a CSTR, evolution of a batch reaction would be able to reflect the dynamic behavior occurring at the corresponding bifurcation conditions. The phenomenon shown above thus illustrates that the closed ferrioin-BZ reaction evolves through two bifurcation regimes, where the first bifurcation regime occurs as soon as spontaneous oscillations begin.

BrMA has been suggested to play an essential role in the development of complex oscillations in the cerium-BZ reaction,<sup>42,45</sup> in which transient complex oscillations would not occur until the concentration of BrMA has reached a certain level.<sup>37–39</sup> However, in the system studied here the first bifurcation regime appeared right after the start of spontaneous oscillations, in which there was an unlikely large amount of BrMA in the solution. Therefore, BrMA may not play a critical role in the occurrence of the first bifurcation sequence in this study, or alternatively, the ferrioin-BZ system is so sensitive to the production of  $\text{Br}^-$  that it does not require the presence of a large amount of BrMA. To shed light on the above issue, a series of experiments in the initial presence of BrMA were conducted in which BrMA was prepared by adding different amounts of bromide into the reaction mixture. These studies illustrated that when  $[\text{BrMA}] = 0.001 \text{ M}$  the total numbers of mixed-mode oscillations within the first bifurcation regime were doubled and even the pattern of one large and two small peaks per cycle ( $1^2$ ) could be observed there. In contrast, no significant influence on oscillations of the second bifurcation sequence was seen. Further increase of BrMA concentration ( $>0.0025 \text{ M}$ ) prolonged the first bifurcation regime dramatically, but eliminated the second bifurcation regime. These results illustrate that BrMA still plays an important role in the complex oscillations in the ferrioin-catalyzed BZ reaction; however, the two bifurcation regimes are likely governed by different mechanisms.

To gain further insight into the dynamics of the two bifurcation regimes, initial compositions of the reaction solution were adjusted systematically in the following experiments. In Figure 2, the concentration of ferrioin was decreased gradually, while all other reaction conditions were kept the same as those in Figure 1. Note that Figure 2a shows the first 1100 s of the corresponding time series collected in Figure 2b. Mixed-mode oscillations including patterns of one large and two small peaks per cycle ( $1^2$ ) can be seen in the time series Figure 2a(I), where



**Figure 2.** Time series of BZ reaction under different initial concentrations of ferroin: (I)  $10.0 \times 10^{-4}$  M, (II)  $4.0 \times 10^{-4}$  M, and (III)  $2.0 \times 10^{-4}$  M. Other reaction conditions are the same as those in Figure 1. Part a plots the first 1100 s of the corresponding time series in (b).

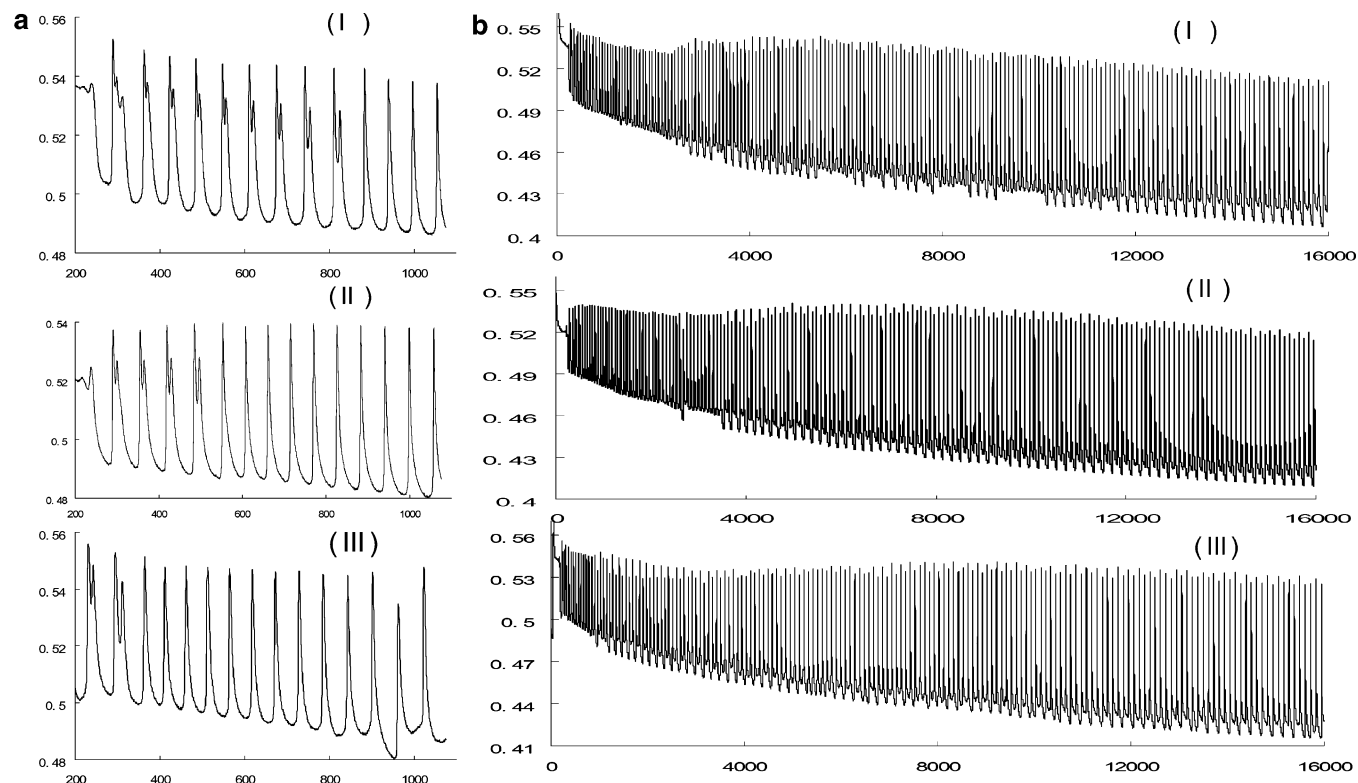
[ferroin] =  $10.0 \times 10^{-4}$  M. These mixed-mode oscillations become simpler and last for a shorter period of time in the time series Figure 2a(II), in which ferroin concentration was decreased to  $5.0 \times 10^{-4}$  M. The first bifurcation regime diminished completely in the time series Figure 2a(III) when ferroin concentration was decreased to  $2.0 \times 10^{-4}$  M. As shown in Figure 2b, the second group of complex oscillations in both series I and II did not begin until the first bifurcation regime disappeared more than 25 min. In contrast to the first bifurcation sequence, complexities of the second bifurcation regime (see Figure 2b) were actually enhanced as the result of decreasing the concentration of ferroin. The second bifurcation regime also lasted longer at lower ferroin concentration, which was, again, opposite what happened to the first bifurcation regime.

Figure 3 shows effects of MA concentration on the two bifurcation regimes, in which the initial concentration of MA is (I) 0.40 M, (II) 0.30 M, and (III) 0.20 M. Other reaction conditions are the same as those in Figure 1, i.e.,  $[\text{H}_2\text{SO}_4] = 0.38$  M,  $[\text{ferroin}] = 5.0 \times 10^{-4}$  M, and  $[\text{BrO}_3^-] = 0.10$  M. Again, Figure 3a presents the first 1100 s of the corresponding time series collected in Figure 3b. Results in Figure 3a illustrate that the first bifurcation regime lasted for a shorter period of time as the concentration of MA was decreased. Meanwhile, the complexity of these mixed-mode oscillations also appears to be reduced as the pattern of one large and two small peaks per cycle ( $1^2$ ) can be seen at  $[\text{MA}] = 0.4$  M but not at  $[\text{MA}] = 0.3$  or 0.2 M. When the concentration of MA became smaller than 0.1 M, the first bifurcation regime disappeared. Under all three conditions characterized here, on the other hand, there was no dramatic change in the behavior of the second bifurcation regime, although complex oscillations in the second bifurcation regime appeared to become slightly irregular at higher MA concentration. The second bifurcation regime in all three cases continued for about the same amount of time ( $\approx 300$  min).

Influences of bromate concentration on the above sequential bifurcation regimes are summarized in Figure 4, in which  $[\text{BrO}_3^-]$  is (I) 0.11 M, (II) 0.09 M, (III) 0.07 M, and (IV) 0.06

M. Other reaction conditions are the same as those in Figure 1. Initially, both the complexity and lifetime of the first bifurcation regime were increased as bromate concentration was decreased from 0.11 M in series I to 0.09 M in series II. Interestingly, in the time series Figure 4a(III) a new small amplitude peak developed at the bottom of two consecutive large peaks while the original small peak of the mixed-mode oscillations could still, though barely, be seen. Careful examination of the time series Figure 4b(III) illustrates that the insertion of the new small peak is due to the two bifurcation regimes merging under this set of reaction conditions. If the concentration of bromate was decreased still (see time series IV), these new peaks occurring in the time series Figure 4a(III) disappeared again. Such a result was because the second bifurcation regime diminished under those conditions (see the complete time series Figure 4b(IV)). Notably, when bromate concentration was adjusted as the only variable, the second bifurcation regime disappeared first. Figure 4 also indicates that there was an optimum range of bromate concentration for the development of both the first and the second bifurcation regimes in the ferroin-BZ reaction. Such a phenomenon is somehow different from what was reported in the cerium-catalyzed BZ reaction, in which increasing bromate concentration seemed to always enhance the complexity of transient oscillations.<sup>37</sup>

Figure 5 illustrates the influence of the concentration of sulfuric acid on the ferroin-BZ reaction, in which Figure 5a presents the first 1800 s of the corresponding time series collected in Figure 5b. Again, all reaction conditions were kept the same as those in Figure 1, except that  $\text{H}_2\text{SO}_4$  concentration was adjusted to 0.30 M in (I) and 0.2 M in (II). As shown in Figure 5a(I), the first bifurcation regime lasted for a longer period of time than that in Figure 1 in which  $[\text{H}_2\text{SO}_4] = 0.38$  M. Complex oscillations in the second bifurcation regime also became more irregular, in which period-2 oscillations mingled with other modes of oscillations such as oscillations of one small and two large peaks per cycle. Careful examination of the time



**Figure 3.** Time series of BZ reaction under different initial concentrations of MA: (I) 0.40 M, (II) 0.30 M, and (III) 0.20 M. Other reaction conditions are the same as those in Figure 1. Part a plots the first 1100 s of the corresponding time series in (b).

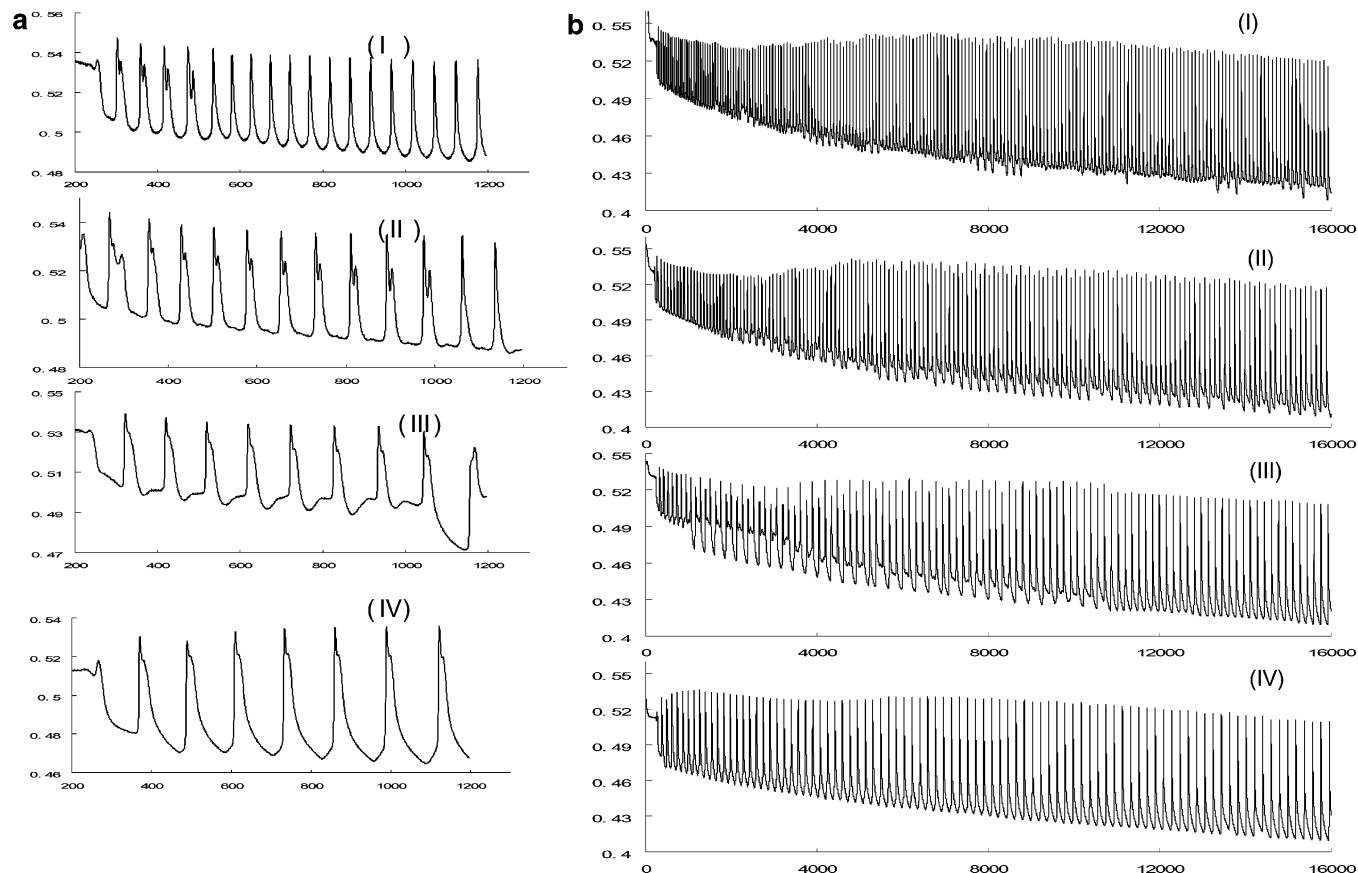


**Figure 4.** Time series of BZ reaction under different initial concentrations of bromate: (I) 0.11 M, (II) 0.09 M, (III) 0.07 M, and (IV) 0.06 M. Other reaction conditions are the same as those in Figure 1. Part a plots the first 1200 s of the corresponding time series in (b).

series Figure 5b(I) indicates that the two bifurcation regimes had already emerged here, in which large amplitude oscillations underwent a bifurcation while the original mixed-mode oscillations were still there (at  $t \approx 1000$  s). As sulfuric acid concentration was decreased further to 0.2 M, only one bifurcation regime was achieved in the time series Figure

Figure 5b(I) indicates that the two bifurcation regimes had already emerged here, in which large amplitude oscillations underwent a bifurcation while the original mixed-mode oscillations were still there (at  $t \approx 1000$  s). As sulfuric acid concentration was decreased further to 0.2 M, only one bifurcation regime was achieved in the time series Figure

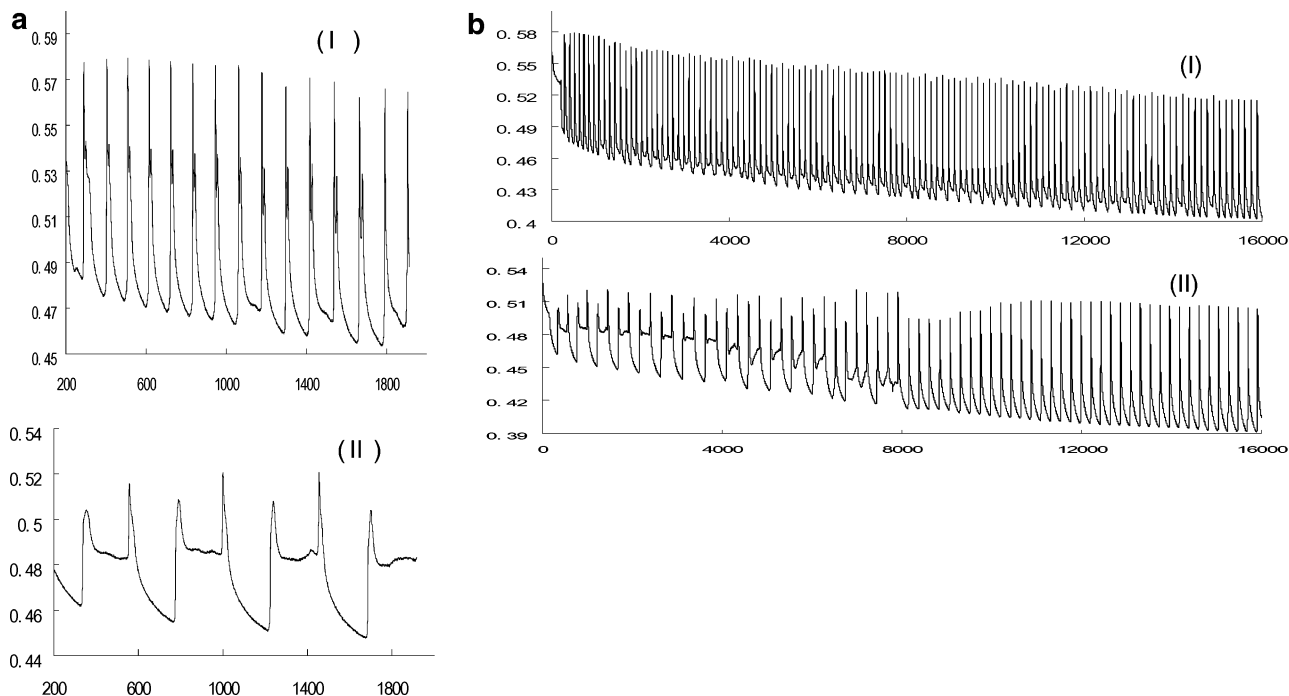


**Figure 5.** Time series of BZ reaction under different initial concentrations of sulfuric acid: (I) 0.30 M and (II) 0.20 M. Other reaction conditions are the same as those in Figure 1. Part a plots the first 1800 s of the corresponding time series in (b).

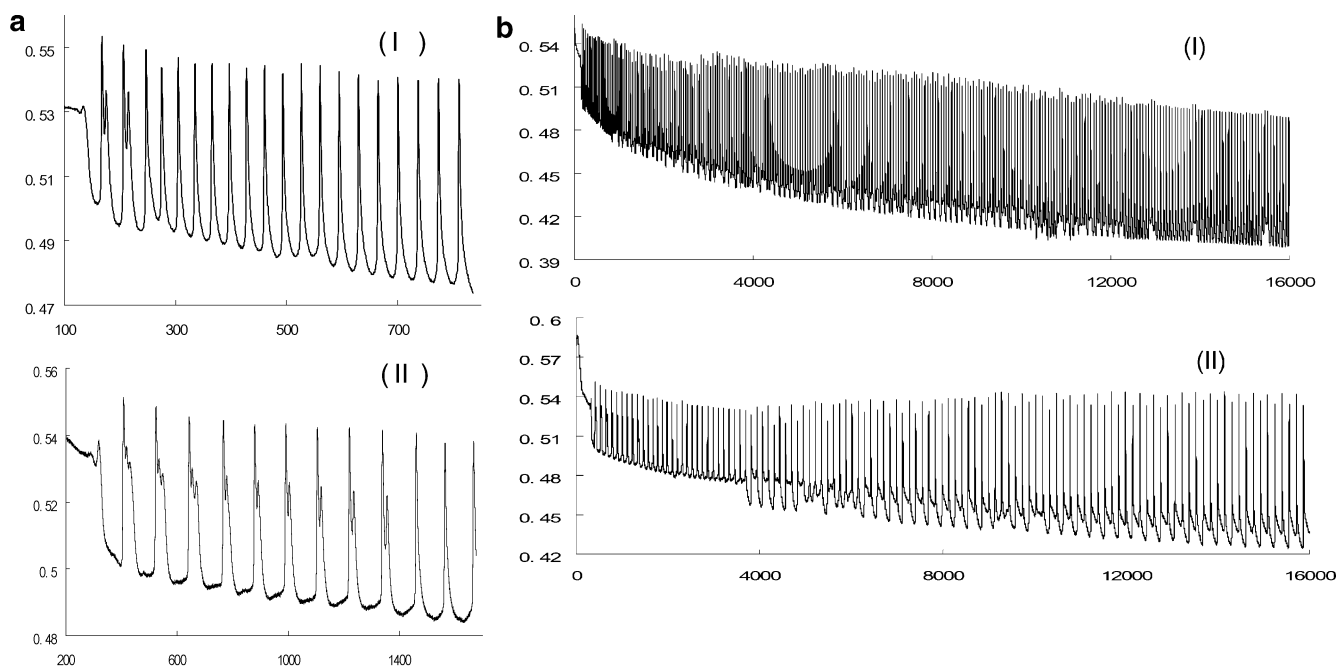


**Figure 6.** Time series of BZ reaction achieved under different reaction temperatures: (I) 25.0 °C and (II) 15.0 °C. Other reaction conditions are the same as those in Figure 1. (a) and (b) are the results collected within different time intervals.

5b(II), which looks like the overlap of the two bifurcation regimes.

In Figure 6 reaction temperature was characterized as the only variable while all other reaction conditions were kept the same as those in Figure 1. When the temperature was increased to 25.0 °C, the total numbers of complex oscillations within the first bifurcation regime were reduced to two. If the temperature was decreased from the reference experiment shown in Figure 1, the first bifurcation sequence became richer and lasted longer as shown in the time series Figure 6a(II), where not only the pattern of one large and one small peak per cycle ( $1^1$ ) but also oscillations of one large and two small peaks per cycle ( $1^2$ ) can be seen. In contrast, complex oscillations in the second

bifurcation regime appear to be more complicated at higher reaction temperature. The opposite response to temperature change further indicates that complex oscillations in the two bifurcation regimes are governed by different reaction mechanisms.

#### 4. Computational Results

As discussed earlier, Keki and co-workers suggested that reactions between ferriin and bromide and between ferroin and  $\text{HBrO}_2$ ,  $\text{HOBr}$ ,  $\text{Br}_2$ , etc. shall also be considered when simulating the ferroin-catalyzed BZ system.<sup>35</sup> Working from the same viewpoint, Strizhak and co-workers proposed a model by

TABLE 1<sup>a</sup>

no.	reaction	rate const
1	$\text{Br}^- + \text{BrO}_3^- + 2\text{H}^+ \rightarrow \text{HOBr} + \text{HBrO}_2$	1.28
2	$\text{HOBr} + \text{HBrO}_2 \rightarrow \text{Br}^- + \text{BrO}_3^- + 2\text{H}^+$	3.3
3	$\text{HBrO}_2 + \text{Br}^- + \text{H}^+ \rightarrow 2\text{HOBr}$	$1.6 \times 10^6$
4	$2\text{HOBr} \rightarrow \text{HBrO}_2 + \text{Br}^- + \text{H}^+$	$2 \times 10^{-5}$
5	$\text{HOBr} + \text{Br}^- + \text{H}^+ \rightarrow \text{Br}_2 + \text{H}_2\text{O}$	$1.84 \times 10^9$
6	$\text{Br}_2 + \text{H}_2\text{O} \rightarrow \text{HOBr} + \text{Br}^- + \text{H}^+$	2
7	$2\text{HBrO}_2 \rightarrow \text{BrO}_3^- + \text{HOBr} + \text{H}^+$	3000
8	$\text{BrO}_3^- + \text{HOBr} + \text{H}^+ \rightarrow 2\text{HBrO}_2$	$6.0 \times 10^{-9}$
9	$\text{BrO}_3^- + \text{HBrO}_2 + \text{H}^+ \rightarrow 2\text{BrO}_2 + \text{H}_2\text{O}$	40
10	$2\text{BrO}_2 + \text{H}_2\text{O} \rightarrow \text{BrO}_3^- + \text{HBrO}_2 + \text{H}^+$	$4.2 \times 10^7$
11	$\text{MA} + \text{Br}_2 \rightarrow \text{BrMA} + \text{Br}^- + \text{H}^+$	28.65
12	$\text{MA} + \text{HOBr} \rightarrow \text{BrMA} + \text{H}_2\text{O}$	8.2
13	$\text{BrMA} + \text{HOBr} \rightarrow \text{product}$	0.1
14	$2\text{BrMA} + \text{H}_2\text{O} \rightarrow \text{BrMA} + \text{BrTTA}$	$1 \times 10^8$
15	$\text{BrMA} + \text{BrO}_2 + \text{H}_2\text{O} \rightarrow \text{HBrO}_2 + \text{BrTTA}$	$5 \times 10^{11}$
16	$\text{BrMA} + \text{MA} + \text{H}_2\text{O} \rightarrow \text{MA} + \text{BrTTA}$	$1 \times 10^9$
17	$\text{MA} + \text{BrO}_2 \rightarrow \text{product}$	$5 \times 10^9$
18	$\text{MA} + \text{BrO}_3^- + \text{H}^+ \rightarrow \text{BrO}_2 + \text{product}$	32
19	$\text{BrTTA} \rightarrow \text{Br}^- + \text{product}$	1
20	$\text{BrMA} + \text{BrO}_3^- + \text{H}^+ \rightarrow \text{BrO}_2 + \text{BrTTA}$	32
21	$\text{Fe}^{2+} + \text{BrO}_2 + \text{H}^+ \rightarrow \text{Fe}^{3+} + \text{HBrO}_2$	$7 \times 10^7$
22	$2\text{Fe}^{2+} + \text{BrO}_3^- + 3\text{H}^+ \rightarrow 2\text{Fe}^{3+} + \text{HBrO}_2 + \text{H}_2\text{O}$	0.256
23	$2\text{Fe}^{2+} + \text{HBrO}_2 + 2\text{H}^+ \rightarrow 2\text{Fe}^{3+} + \text{HOBr} + \text{H}_2\text{O}$	1.6
24	$2\text{Fe}^{2+} + \text{HOBr} + \text{H}^+ \rightarrow 2\text{Fe}^{3+} + \text{Br}^- + \text{H}_2\text{O}$	$5 \times 10^{-3}$
25	$2\text{Fe}^{2+} + \text{Br}_2 + \text{H}^+ \rightarrow 2\text{Fe}^{3+} + 2\text{Br}^-$	100
26	$2\text{Fe}^{3+} + 2\text{Br}^- \rightarrow 2\text{Fe}^{2+} + \text{Br}_2 + \text{H}^+$	b
27	$\text{Fe}^{3+} + \text{MA} \rightarrow \text{Fe}^{2+} + \text{MA} + \text{H}^+$	$1 \times 10^{-2}$
28	$\text{Fe}^{3+} + \text{BrMA} \rightarrow \text{Fe}^{2+} + \text{BrMA} + \text{H}^+$	20
29	$\text{Fe}^{2+} + \text{BrMA} + \text{H}^+ \rightarrow \text{Fe}^{3+} + \text{BrMA}$	$5 \times 10^7$

<sup>a</sup>  $[\text{H}^+] = 0.8 \text{ M}$  and  $[\text{H}_2\text{O}_2] = 55.56 \text{ M}$  are included in the rate constants. Discussion regarding the election of these rate constants can be found in ref 35. <sup>b</sup> See ref 35.

incorporating those reactions suggested by Keki et al. to describe complex oscillations in the ferriin-catalyzed BZ reaction observed in a CSTR.<sup>36</sup> Their model, listed in Table 1, consists of 12 reagent species (variables) and 29 steps. Since the model successfully reproduced the bifurcation sequence observed in the CSTR, it was employed here as a prototype model to simulate the ferriin-BZ reaction in a batch reactor. When the model was directly applied to simulate the closed ferriin-catalyzed BZ reaction, no complex oscillations could be seen under the same conditions as employed in our experiments. Indeed, no complex phenomena could be achieved in the modeling even when initial concentrations of all reactants were adjusted over a broad range.

To obtain transient complex oscillations, three rate constants, namely,  $k_{15}$ ,  $k_{21}$ , and  $k_{29}$ , have been adjusted here.  $k_{15}$  was increased to be 60 times higher while  $k_{21}$  and  $k_{29}$  became, respectively, 7 and 40 times smaller than those values used by Strizhak and co-workers.<sup>36</sup> Discussions regarding the selection of other rate constants can be found in the original work published by Strizhak and co-workers.<sup>36</sup> Our numerical simulations illustrated that the complex dynamic behavior of the ferriin-catalyzed BZ reaction was particularly sensitive to variations of the following rate constants:  $k_1$ ,  $k_{15}$ ,  $k_{19}$ ,  $k_{21}$ ,  $k_{22}$ , and  $k_{29}$ . For example, both increasing and decreasing the value of  $k_1$  from that used in this study reduced the complexity of BZ oscillations. Qualitatively the same kinds of influences were observed when rate constants  $k_{15}$ ,  $k_{19}$ ,  $k_{21}$ ,  $k_{22}$ , and  $k_{29}$  were characterized individually.

An example of transient complex oscillations calculated from the model is presented in Figure 7, in which the initial concentration of bromate is (a) 0.11 M, (b) 0.09 M, (c) 0.07 M, and (d) 0.06 M. Initial values of other reactants in the above calculations matched those used in experiments. Similar to the experimental observation (see Figure 4), when the initial

concentration of bromate was too low, such as 0.06 M in the time series Figure 7d, no complex oscillations occurred. On the other hand, as the bromate concentration was increased, complex oscillations became more complicated. Notably, in both parts a and b of Figure 7, the small peak of the period-doubled oscillations become invisible even under logarithmic scale at  $t \approx 2000 \text{ s}$ , implying that period-doubled oscillations tend to cease here. Beyond that point, the small peak revived and became more and more prominent in time. From a dynamic point of view, such a scenario implicates that a reverse period-doubling bifurcation takes place at  $t \approx 1800 \text{ s}$  to lead the system back to simple oscillations, which is then followed by another forward period-doubling bifurcation leading the system to complex oscillations. In Figure 7c, the first group of period-doubled oscillations, which appeared before  $t = 1800 \text{ s}$ , disappeared spontaneously, while period-doubled oscillations which resembled the second part of period-doubled oscillations shown in Figure 7a,b were still there. This suggests that period-doubled oscillations appearing before  $t \approx 1800 \text{ s}$  may correspond to the first bifurcation regime observed in experiments, whereas complex oscillations appearing after  $t \approx 1800 \text{ s}$  correspond to the second bifurcation regime. Unfortunately, we failed to obtain a few simple oscillations around  $t = 1800 \text{ s}$ , even though rate constants as well as initial values of reactants had been tuned delicately. In addition, as opposed to experimental observation, the first group of period-doubled oscillations seen in the above modeling does not appear as soon as spontaneous oscillations begin. Further improvement of the model will be conducted in our future work.

As discussed earlier, an essential difference between the FKN mechanism and the model proposed by Strizhak and co-workers is that Strizhak and co-workers considered reactions between ferriin/ferriin and HOBr,  $\text{Br}_2$ ,  $\text{HBrO}_2$ , etc.<sup>34,36</sup> To examine the importance of those new steps in the development of complex oscillations, we have respectively adjusted rate constants  $k_{22}$ ,  $k_{23}$ ,  $k_{24}$ ,  $k_{25}$ , and  $k_{26}$ . Our calculations illustrated that variation of  $k_{22}$  had significant effects on complex oscillations. Indeed, complex oscillations could be obtained only when  $k_{22}$  was within a proper range. However, when  $k_{23}$ ,  $k_{24}$ , and  $k_{26}$  were changed to 0, which corresponded to excluding those reactions from the proposed mechanism, there was no change at all in the complex oscillation pattern. When  $k_{25}$  was adjusted to 0, complex oscillations became slightly simpler. For example, oscillations shown in Figure 7a would become those shown in Figure 7b as  $k_{25}$  was changed to 0.

## 5. Conclusions

In this study, the ferriin-catalyzed BZ reaction was investigated in a closed system and was found to evolve through two bifurcation regimes. To the best of our knowledge, it is the first example that a closed chemical system can exhibit such complicated reaction dynamics. The two bifurcation regimes exhibited qualitatively different dependence on initial compositions of the reaction mixture and reaction temperature, suggesting that complex oscillations in the two bifurcation regimes are likely governed by different reaction processes. Such a conclusion is further supported by the opposite responses of the two bifurcation regimes to the addition of BrMA: increasing the initial concentration of BrMA to above 0.0025 M dramatically prolonged the first bifurcation regime; yet adverse effects on the second bifurcation regime took place and the second bifurcation regime diminished if  $[\text{BrMA}] > 0.005 \text{ M}$ . Under suitable reaction conditions, however, the two bifurcation regimes can merge to produce new modes of oscillations such as those shown in Figure 5b(II).

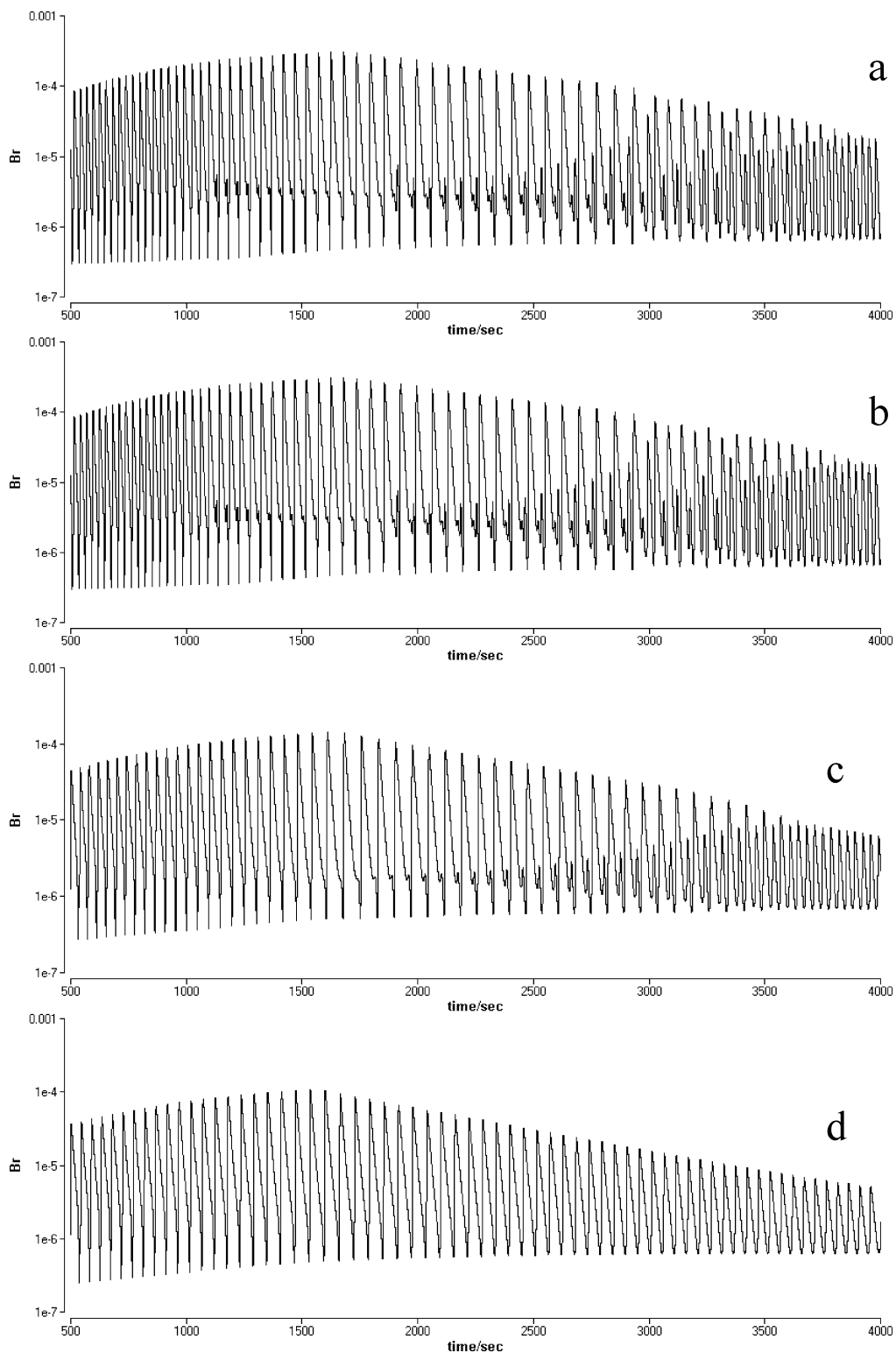
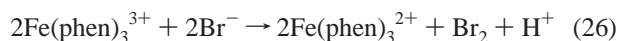
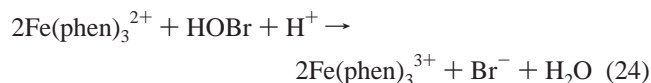
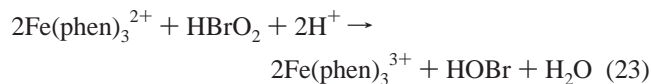


**Figure 7.** Time series of BZ oscillations calculated at different initial concentrations of  $\text{BrO}_3^-$ : (a) 0.11 M, (b) 0.09 M, (c) 0.07 M, and (d) 0.06 M. Rate constants used in this study are listed in Table 1. Initial concentrations of other reactants are the same as used in experiments. Initial values of the intermediate species are all set to 0.

Numerical simulations with a model developed initially by Strizhak and co-workers have successfully reproduced transient complex oscillations observed in experiments. The bifurcation sequence in the modeling also appears to consist of two regimes, in which the first part of period-doubled oscillations disappears simultaneously as a result of varying reaction parameters, i.e., decreasing  $\text{BrO}_3^-$  concentration. Unfortunately, no simple oscillations (i.e., one peak per period) were obtained between the two bifurcation regimes, despite adjustment of rate constants

as well as initial values of all reactants over a broad range. It is interesting to point out that we found that the above model was also capable of supporting sequential oscillations under certain reaction conditions, although no such behavior has ever been observed in our experiments. Whether it represents another theory, complementing the radical mechanism suggested by Försterling et al., to explain the sequential oscillations observed in the cerium-catalyzed BZ reaction<sup>46</sup> will be explored in our future work.

Numerical simulations conducted in this study also illustrated that eliminating the following three reaction steps from the model listed in Table 1 had no influence on transient complex oscillations:



Therefore, the mechanism proposed by Strizhak and co-workers could be simplified into a model consisting of only 26 steps.

**Acknowledgment.** This work is supported by the National Science and Engineering Research Council of Canada (NSERC) and Canadian Foundation for Innovation (CFI). Q.G. thanks NSFC (20103010) and EYTP of China for financial support.

### References and Notes

- (1) *Oscillations and Traveling Waves in Chemical Systems*; Field, R. J., Burger, M., Eds.; Wiley-Interscience: New York 1985.
- (2) Scott, S. K. *Chemical Chaos*; Oxford University Press: Oxford, UK, 1991.
- (3) Epstein, I. R.; Pojman, J. A. *An Introduction to Nonlinear Chemical Dynamics*; Oxford University Press: Oxford, UK, 1998.
- (4) *Chemical Waves and Patterns*; Kapral, R., Showalter, K., Eds.; Kluwer Academic Publishers: Netherlands, 1995.
- (5) Goldbeter, A. *Biochemical Oscillations and Cellular Rhythms*; Cambridge University Press: Cambridge, UK, 1996.
- (6) Epstein, I. R.; Showalter, K. *J. Phys. Chem.* **1996**, *100*, 13132.
- (7) Farage, V. J.; Janjic, D. *Chem. Phys. Lett.* **1982**, *93*, 621.
- (8) Simoyi, R. H.; Manyonda, M.; Masere, J.; Mtambo, M.; Ncube, I.; Patel, H.; Epstein, I. R.; Kustin, K. *J. Phys. Chem.* **1991**, *95*, 770.
- (9) Rabai, G.; Epstein, I. R. *J. Am. Chem. Soc.* **1992**, *114*, 1529–1530.
- (10) Epstein, I. R.; Kustin, K.; Simoyi, R. H. *J. Phys. Chem.* **1992**, *96*, 5852.
- (11) Simoyi, R. H.; Epstein, I. R.; Kustin, K. *J. Phys. Chem.* **1994**, *98*, 551.
- (12) Schreiber, I.; Hung, Y.-F.; Ross, J. *J. Phys. Chem.* **1996**, *100*, 8556.

- (13) Hauser, M. J. B.; Olsen, L. F.; Bronnikova, T. V.; Schaffer, W. M. *J. Phys. Chem. B* **1997**, *101*, 5075.
- (14) Kurin-Csörgei, K.; Szalai, I.; Körös, E. *React. Kinet. Catal. Lett.* **1995**, *54*, 217.
- (15) Masere, J.; Stewart, F.; Meehan, T.; Pojman, J. A. *Chaos* **1999**, *9*, 315.
- (16) Horvath, A. K.; Nagypal, I.; Epstein, I. R. *J. Am. Chem. Soc.* **2002**, *124*, 10956.
- (17) Krüger, F.; Nagy-Ungvarai, Zs.; Müller, S. C. *Physica D* **1995**, *84*, 95.
- (18) Maselko, J.; Showalter, K. *Nature* **1989**, *339*, 609.
- (19) Vanag, V. K.; Zhabotinsky, A. M.; Epstein, I. R. *J. Phys. Chem. A* **2000**, *104*, 11566.
- (20) Wang, J.; Kádár, S.; Jung, P.; Showalter, K. *Phys. Rev. Lett.* **1999**, *82*, 855.
- (21) Amemiya, T.; Kettunen, P.; Kádár, S.; Yamaguchi, T.; Showalter, K. *Chaos* **1998**, *8*, 872.
- (22) Steinbock, O.; Zykov, V. S.; Müller, S. C. *Nature* **1993**, *366*, 322.
- (23) Manz, N.; Müller, S. C.; Steinbock, O. *J. Phys. Chem. A* **2000**, *104*, 5895.
- (24) Kaern, M.; Menzinger, M. *J. Phys. Chem. A* **2002**, *106*, 4897.
- (25) Ouyang, Q.; Swinney, H. L.; Li, G. *Phys. Rev. Lett.* **2000**, *84*, 1047.
- (26) Sevcikova, H.; Kosek, J.; Marek, M. *J. Phys. Chem.* **1996**, *100*, 1666.
- (27) Manz, N.; Grun, B. T.; Steinbock, O. *J. Phys. Chem. A* **2003**, *107*, 11008.
- (28) Bamforth, J. R.; Toth, R.; Gaspar, V.; Scott, S. K. *Phys. Chem. Chem. Phys.* **2002**, *4*, 1299.
- (29) Hudson, J. L.; Hart, M.; Marinko, D. *J. Chem. Phys.* **1979**, *71*, 6104.
- (30) Roux, J. C.; Simonyi, R. H.; Swinney, H. L. *Physica D* **1983**, *8*, 257.
- (31) Roux, J. C.; DeKepper, P.; Boissonate, J. *Phys. Lett. A* **1983**, *97*, 168.
- (32) Ali, F.; Menzinger, M. *J. Phys. Chem.* **1997**, *101*, 2304.
- (33) Ruoff, P. *J. Phys. Chem.* **1993**, *97*, 6405.
- (34) Field, R. J.; Körös, E.; Noyes, R. M. *J. Am. Chem. Soc.* **1972**, *94*, 8649.
- (35) Keki, S.; Magyar, I.; Beck, M. T.; Gaspar, V. *J. Phys. Chem.* **1992**, *96*, 1725.
- (36) Kalishin, E. Yu.; Goncharenko, M. M.; Khavrus, V. A.; Strizhak, P. E. *Kinet. Catal.* **2002**, *43*, 256.
- (37) Wang, J.; Sørensen, P. G.; Hynne, F. *J. Phys. Chem.* **1994**, *98*, 725.
- (38) Wang, J.; Sørensen, P. G.; Hynne, F. *Z. Phys. Chem.* **1995**, *192*, 63.
- (39) John, B. R.; Scott, S. K.; Thompson, B. W. *Chaos* **1997**, *7*, 350.
- (40) Strizhak, P. E.; Kawczynski, A. *Ž. J. Phys. Chem.* **1995**, *99*, 10830.
- (41) Field, R. J.; Forsterling, H.-D. *J. Phys. Chem.* **1986**, *90*, 5400.
- (42) Györgyi, L.; Rempe, S. L.; Field, R. J. *J. Phys. Chem.* **1991**, *95*, 3159.
- (43) Goryachev, A.; Kapral, R. *Int. J. Bif. Chaos* **1999**, *9*, 2243.
- (44) Goryachev, A.; Kapral, R. *Phys. Rev. E* **1996**, *54*, 5469.
- (45) Györgyi, L.; Field, R. *Nature* **1992**, *355*, 808.
- (46) Försterling, H. D.; Murányi, S.; Noszticzius, S. *Z. J. Phys. Chem.* **1990**, *94*, 2915.